Fermi National Accelerator Laboratory

FERMILAB-FN-603

# Detection of $H^0 \rightarrow \gamma\gamma$ by the SDC Detector

W. Wu, A. Beretvas, D. Green and J. Marraffino

*Fermi National Accelerator Laboratory*
*P.O. Box 500, Batavia, Illinois 60510*

April 1993

Operated by Universities Research Association Inc. under Contract No. DE-AC02-76CHO3000 with the United States Department of Energy

## Disclaimer

# Detection of $H^0 \rightarrow \gamma\gamma$ by the SDC Detector

W. Wu, A. Beretvas, D. Green, and J. Marraffino

Fermi National Accelerator Laboratory, Batavia, Illinois, 60510.

## Introduction

A light Higgs ($M_{Higgs} < 80$ GeV) will almost certainly be found at LEP II before the SSC turns on. An intermediate mass Higgs($130 < M_{Higgs}$ 180 GeV) can be studied by the decay $H \rightarrow Z^0 Z^* \rightarrow$ 4 leptons (here * indicates a virtual particle). A heavy Higgs ($M_{Higgs} > 180$ GeV) can be studied using the decay to $Z^0$ $Z^0 \rightarrow$ 4 leptons. In this paper we will investigate the low mass region($80 < M_{Higgs} < 130$ GeV). We will look for the decay $H \rightarrow \gamma\gamma$. This decay mode has a relatively small branching ratio ($\approx 10^{-3}$, see Fig. 1), but it is relatively constant over this mass range. What makes observing this decay mode hard is the large QCD backgrounds. Several papers [1], [2],[3] claim that only a detector with exceptional energy resolution will be able to see the $H \rightarrow \gamma\gamma$ signal above the large QCD background. We will investigate the difficulty in seeing the 2 $\gamma$ signal with a "Super Resolution Calorimeter" and also with a "Conventional Calorimeter".

## Generation of events

We use ISAJET version 6.43 to generate both signal and background. To investigate the appropriate mass region we generate 1000 events[1] with a Higgs mass of 80 GeV and an identical number of events at 125 GeV. The Higgs cross section is about 100 pb, and correspondingly the

[1] 5000 events were generated to investigate distributions before cuts.

cross section times branching ratio is 0.1 pb. Thus, the expected number of events produced in a year at the SSC is about 1000. The ISAJET cross section times branching ratio is 0.05 pb at 80 GeV and 0.08 pb at 125 GeV The signal consists of a pair of isolated high $P_T$ photons, and no missing $P_T$. Figure 2 shows a few typical events.

The direct production of photons is perhaps the most serious background and the only one we will consider in our analysis. In this paper we will not consider the background from high energy $\pi^0$'s. The number of such high energy $\pi^0$'s that look like isolated photons needs to be determined. The rate may be high as the number of QCD high $P_T$ jets is vast ($\frac{dR}{d\eta} = 10^6$ Hz for $P_T > 20$ GeV/c)[4]

This "irreducible QCD background" results from both the Born process ($q\,\bar{q} \rightarrow \gamma\gamma$) and the box process ($gg \rightarrow \gamma\gamma$). These backgrounds have been calculated by Dicus and Willenbrock [5]. Based on Ref. [5], Zhu[2] has determined that the cross section (after cuts) for $q\bar{q} \rightarrow \gamma\gamma$ is 59 (14) pb and the corresponding gg cross section is 493 (91) pb. Tao Han has also calculated (after cuts) the Born (34.6 pb) and box (94.7 pb) cross sections [6]. At the present time ISAJET does not simulate the process $gg \rightarrow \gamma\gamma$. Thus our present study will focus only on the $q\bar{q} \rightarrow \gamma\gamma$ background. The corresponding ISAJET cross section is 8.2 pb ( $20 < P_T < 100$ GeV/c). The CDF diphoton cross section is roughly three times what the full QCD predicts [7]. The full QCD calculation is of order $\alpha^2\alpha_s$ and includes lowest order Born, box and bremsstrahlung processes and most next to lowest order processes. The background sample for our study consists of 100,000 events, corresponding to about 1 SSC year. In the next section we will describe 4 cuts that will reduce the signal by roughly a factor of 2 and the background by a factor of 5.

**Cuts**

We use the same four cuts as in ref. [3];

$$| \eta_\gamma | < 2.8\,; \quad | \eta_{\gamma\gamma} | < 3.0\,; \quad E_T(\gamma) > 20.\,GeV\,; \quad | \cos(\theta^*) | < 0.8\,. \tag{1}$$

The corresponding distributions are shown in Fig. 3 (signal) and 4 (background). The angle $\theta^*$ is the polar angle in the $\gamma\gamma$ rest frame. The first two cuts are useful because the Higgs production is more central than the QCD background. The energy plot should have a Jacobian peak at half the mass of the Higgs. That energy scale is much higher than that of the QCD background. The final cut is used because the Higgs is a scalar particle and thus has a flat distribution in $\cos\theta^*$ while the background processes are sharply peaked in the forward and backward directions due to massless particle exchanges in the t and u channels. (This is not visible in Fig. 4.4 because of the $E_T > 20$ GeV cut.)

**Resolution**

The natural width of the low mass Higgs is about 10 MeV and thus the observed width is determined entirely by the resolution of the experiment. The mass resolution is a function of both the energy resolution and the angular resolution:

$$\frac{2\Delta M}{M} = \frac{\Delta E_1}{E_1} \oplus \frac{\Delta E_2}{E_2} \oplus \cot(\frac{\theta}{2})\Delta\theta \tag{2}$$

$E_1$ and $E_2$ are the energies of the two photons and $\theta$ is the opening angle between them. The EM energy resolution is characterized by a stochastic term "a" and a constant term "b".

$$\frac{\Delta E}{E} = \frac{a}{\sqrt{E}} \oplus b \tag{3}$$

We consider two EM calorimeters. The first is called a "Conventional EM calorimeter" and has a stochastic term of 20% and a constant term of 2%. This conventional calorimeter has somewhat poorer energy resolution than the minimal calorimeter requirements given in the SDC TDR [8]. The

second calorimeter has 10 times the energy resolution of the conventional calorimeter (stochastic term of 2% and a constant term of 0.2%). Table 1 gives the stochastic and constant terms for our analysis, the analysis done in the TDR, and that done by Ren-yuan Zhu. The angular resolutions are specified in Table 2. For both the "Conventional" and the "Super" calorimeter we use an energy weighted centroid of the towers ($\Delta\eta = \Delta\phi = 0.05$), as the transverse location of the photon. The corresponding angular resolution is roughly $\delta\phi_1 = \delta\eta_1 = \frac{0.05}{\sqrt{12}}$. This error size is appropriate to a single crystal for an EM detector. Note that the SDC shower maximum resolution is $\pm$ 2.5 mm, which at a radius of 2 m corresponds to an angular error ($\Delta\phi$) of approximately 1.2 mrad. Figure 5 shows the $\eta$ and $\phi$ resolutions for the Shower Maximum (SM) detector that is being designed for the SDC detector.

**Simulation**

After the events are generated we use our simulation program SSCSIM [9, 10, 11] to reconstruct the events and produce histograms and LEGO plots. In order to analyse the events we need to determine the cone size required to cluster the energy deposited in the EM calorimeter by the photons. Figure 6 shows $\frac{dE}{dr}$ for the Conventional calorimeter. The standard considerations apply; if we make the cone too small some of the energy is not observed and our mass resolution is poor. However, if the cone is too large we have included "underlying event" particles into our sample and have degraded the mass resolution. Based on studies of the mass resolution of the Higgs we find that the best choice of radius, for a luminosity of $10^{33}$ cm$^{-2}$ sec$^{-1}$, is 0.2 for the Super resolution calorimeter and 0.3 for the Conventional one. The criteria for finding a cluster have been described [11]. We observe that our jet finding algorithm is very efficient and that we are able to reconstruct about 85% of the events. Figures 7 (80 GeV) and 8 (125 GeV) show the Higgs mass as reconstucted for the two gammas. The mean and sigma for the reconstructed Higgs mass are given in Table 3.

The mass resolution ($\frac{\Delta M}{M}$) at 80 (125) GeV for the Super calorimeter is 2.7 (2.3)%, and for the Conventional calorimeter it is 5.9 (5.1)%.

**Results**

Figure 9.1 (9.2) shows the reconstructed mass from the $q\bar{q} \rightarrow \gamma\gamma$ background for a Super (Conventional) resolution EM calorimeter. We have generated 100,000 events of which about 20,000 have passed all the cuts. Figure 10.1 shows the combined plot of signal(80 GeV) and background for the case of a Super calorimeter. The background has been fitted to a seventh order polynomial.

The curve is a fit to the region (60-71 GeV) and (89-300 GeV). We have excluded 7 bins in the region of the Higgs mass. When the background is subtracted we obtain the curve given in Fig. 10.2. We see that the resulting signal can be fit by a Gaussian. The signal has a mean of 73 GeV with a sigma of 2.2 GeV. We apply the same procedure to find the signals for a Conventional calorimeter. In Figure 11.1 we see that it is now hard to see the raw signal. After subtracting the background the signal has a mean of 71.1 GeV and a sigma of 4.6 GeV (see Figure 10.2). We next show the same figures for a signal at 125 GeV. To obtain the curve for the background we have excluded a region of $\pm$ 9 GeV centered on the Higgs mass. Figures 12.1 (13.1) and 12.2 (13.2) are for the Super resolution (Conventional) calorimeter before and after subtracting backgrounds. These results plus results for the mass resolution are given in Table 3.

**Conclusions**

Angles are important! EM fluctuations limit the accuracy of $\gamma$ pointing. Therefore 10 times better energy resolution cannot be realized as 10 times better mass resolution. Rather, the improvement is roughly a factor of 2 without the construction of a finely segmented transverse detector such as the SDC shower maximum detector. Such a detector is not gracefully constructed in a crystal architecture.

## References


[1] C. Barter *et al.*, "Detection of $H^0 \rightarrow \gamma\gamma$ at the SSC" High Energy Physics in the 1990's, Snowmass 1988, p. 98.

[2] Ren-yuan Zhu, "Limits to the Precision of Electromagnetic Calorimeters" Proceedings of the First International Conference on Calorimetrs in High Energy Physics, (World Scientific) p 25, 1991.

[3] Ren-yuan Zhu, "A High Resolution Barium Fluoride Calorimeter" Calt-68-1656 in Super Collider II, Plenum Press, ed. McAshan, March 1990.

[4] D. Green, "Physics Requirements for LHC/SSC Calorimetry" Fermilab-Conf-91/281.

[5] D. A. Dicus and S. S. D. Willenbrock, Phys. Rev. D **37**, 1801 (1988).

[6] T. Han (private communication).

[7] F. Abe *et al.*, "Measurement of the cross-section for production of two isolated prompt photons in $\overline{\mathrm{p}}\mathrm{p}$ collisions at $\sqrt{s} = 1.8$ TeV." Fermilab-Pub-92-380-E, (Dec. 1992).

[8] Solenoidal Detector Collaboration, Technical Design Report, SDC-92-201, Apr. 1, 1992.

[9] A. Beretvas *et al.*, SSCSIM user guide (internal note SSC-SDC-Fermilab-31).

[10] A. Para, A. Beretvas, K. Denisenko, N. Denisenko, D. Green, H. Iso, W. Wu, and G. P. Yeh, "Jet Energy Resolution of the SDC Detector", Fermilab-TM-1720 (Dec. 6, 1990).

[11] W. Wu, "Updated Capabilities of SSCSIM", (internal note SSC-SDC-Fermilab-99) (1992).

Table 1:

*Stochastic and constant term coefficients*

for EM Barrel and Endcap compartments of the SDC calorimeter

| Reference | Barrel $\mid \eta \mid < 1.4$ | Endcap $1.4 < \mid \eta \mid < 3.0$ |
|---|---|---|
| Super | | |
| a | 0.02 | 0.02 |
| b | 0.002 | 0.002 |
| Conventional | | |
| a | 0.2 | 0.2 |
| b | 0.02 | 0.02 |
| TDR High Performance | | |
| a | 0.09 | 0.14 |
| b | 0.01 | 0.01 |
| TDR Conventional | | |
| a | 0.14 | 0.17 |
| b | 0.01 | 0.01 |
| $BaF_2$ ref. 2 | | |
| a | 0.013 | 0.013 |
| b | 0.005 | 0.005 |

Table 2:

| Angular Resolution | | | |
|---|---|---|---|
| Reference | $\Delta\phi_1$(mrad) | $\Delta\eta_1$(mrad) | $\Delta\theta$(mrad) |
| Super | 14 | 14 | 56 |
| Conventional | 14 | 14 | 56 |
| SDC (SM) | 1.5 | 1.1 | 5.1 |
| TDR High Performance | | | 1. |
| TDR Conventional | | | 1. |
| $BaF_2$ ref. 2 | | | 1. |

Table 3:

| Higgs Mass Resolution | | | | | | |
|---|---|---|---|---|---|---|
| | Higgs Mass (80 GeV/$c^2$) | | | Higgs Mass (125 GeV/$c^2$) | | |
| | Width (GeV/$c^2$) | Mean (GeV/$c^2$) | $\frac{\Delta M}{M}$ | Width (GeV/$c^2$) | Mean (GeV/$c^2$) | $\frac{\Delta M}{M}$ |
| | Signal only | | | | | |
| Conventional | 4.53 | 76.7 | 5.9% | 6.04 | 118.8 | 5.1% |
| Super | 2.08 | 76.6 | 2.7% | 2.76 | 118.9 | 2.3% |
| | Signal - Background | | | | | |
| Conventional | 4.60 | 71.1 | 6.5% | 6.90 | 116.1 | 5.9% |
| Super | 2.22 | 73.0 | 3.0% | 2.66 | 114.7 | 2.3% |

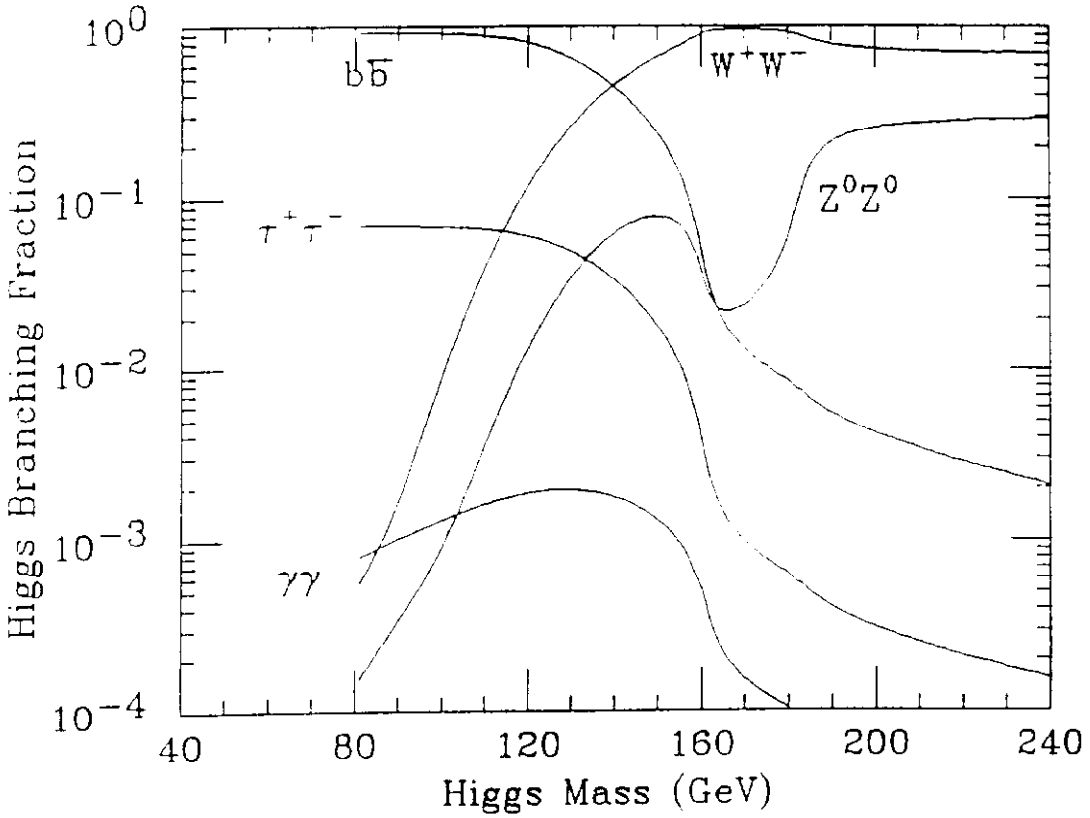


Figure 1: The branching ratio for a Higgs boson into various channels as a function of its mass. (Fig 3-4 from ref. 8)

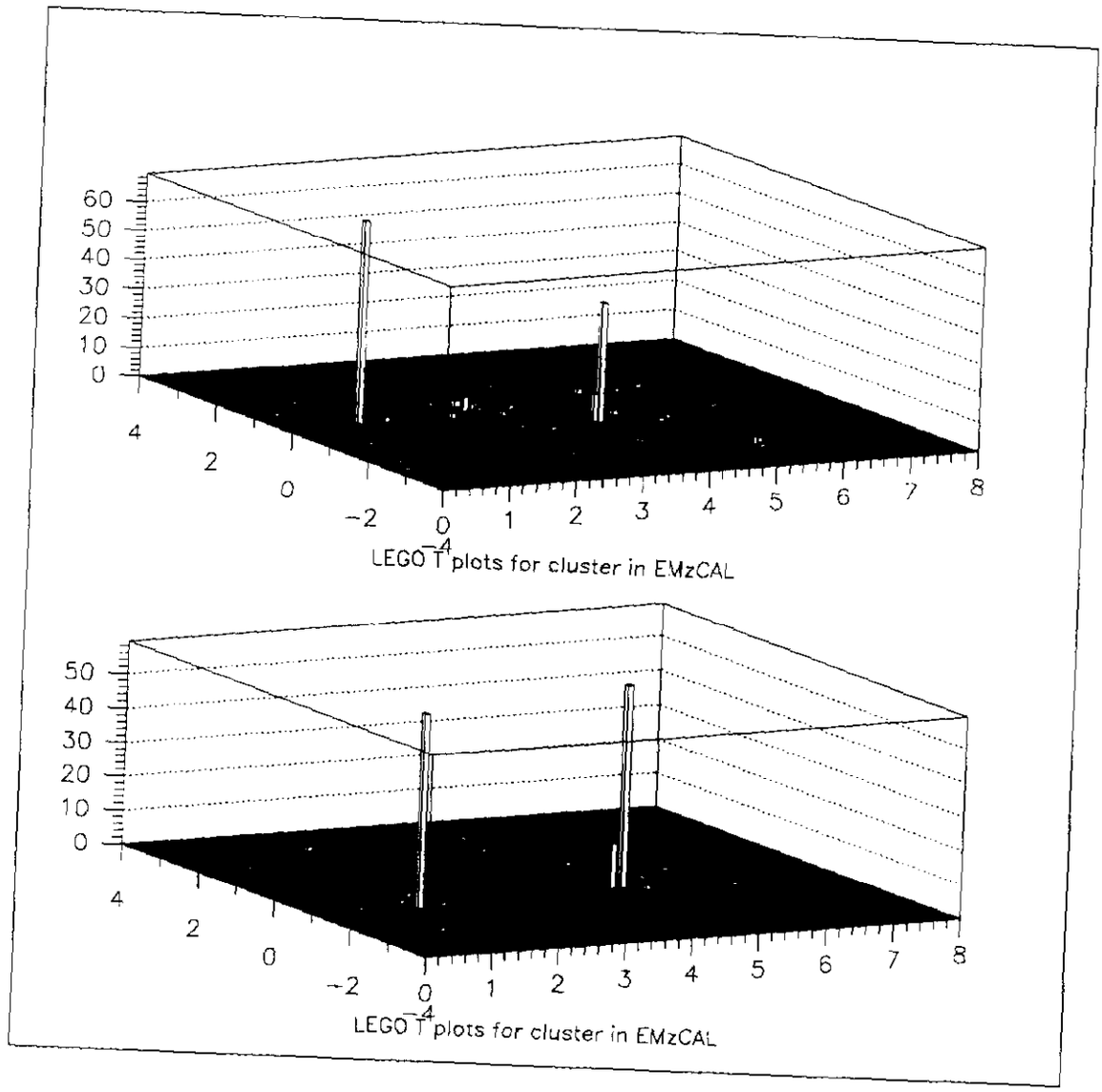


**Figure : 2.1, 2.2 Lego Plots showing $E_T$ (GeV) distributions for typical $H \rightarrow \gamma\gamma$.**

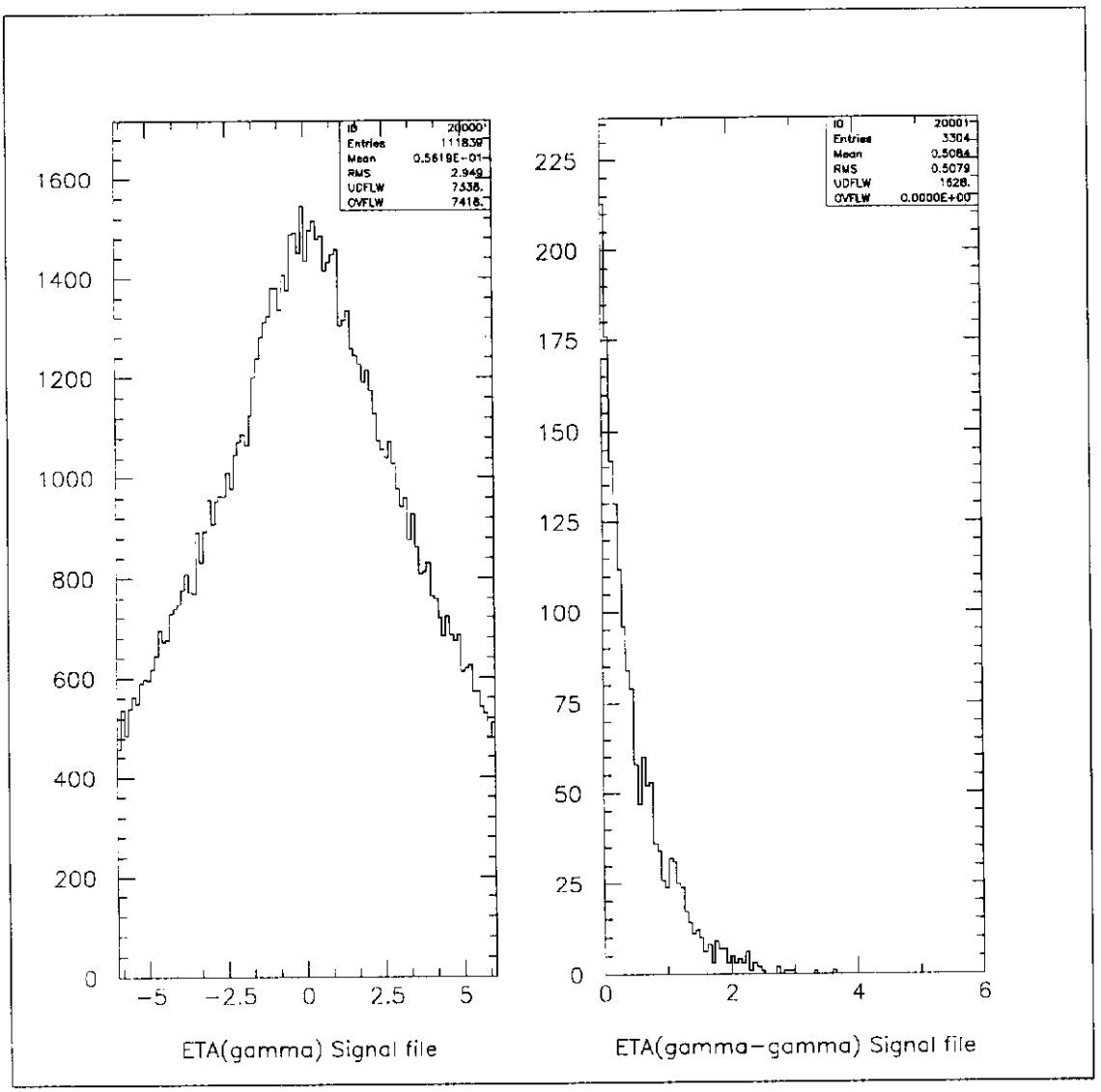


**Figure : 3.1 Distribution of $\eta_\gamma$ for H $\rightarrow \gamma\gamma$ Fig. 3.2 Distribution of $\eta_{\gamma\gamma}$ for H $\rightarrow \gamma\gamma$**

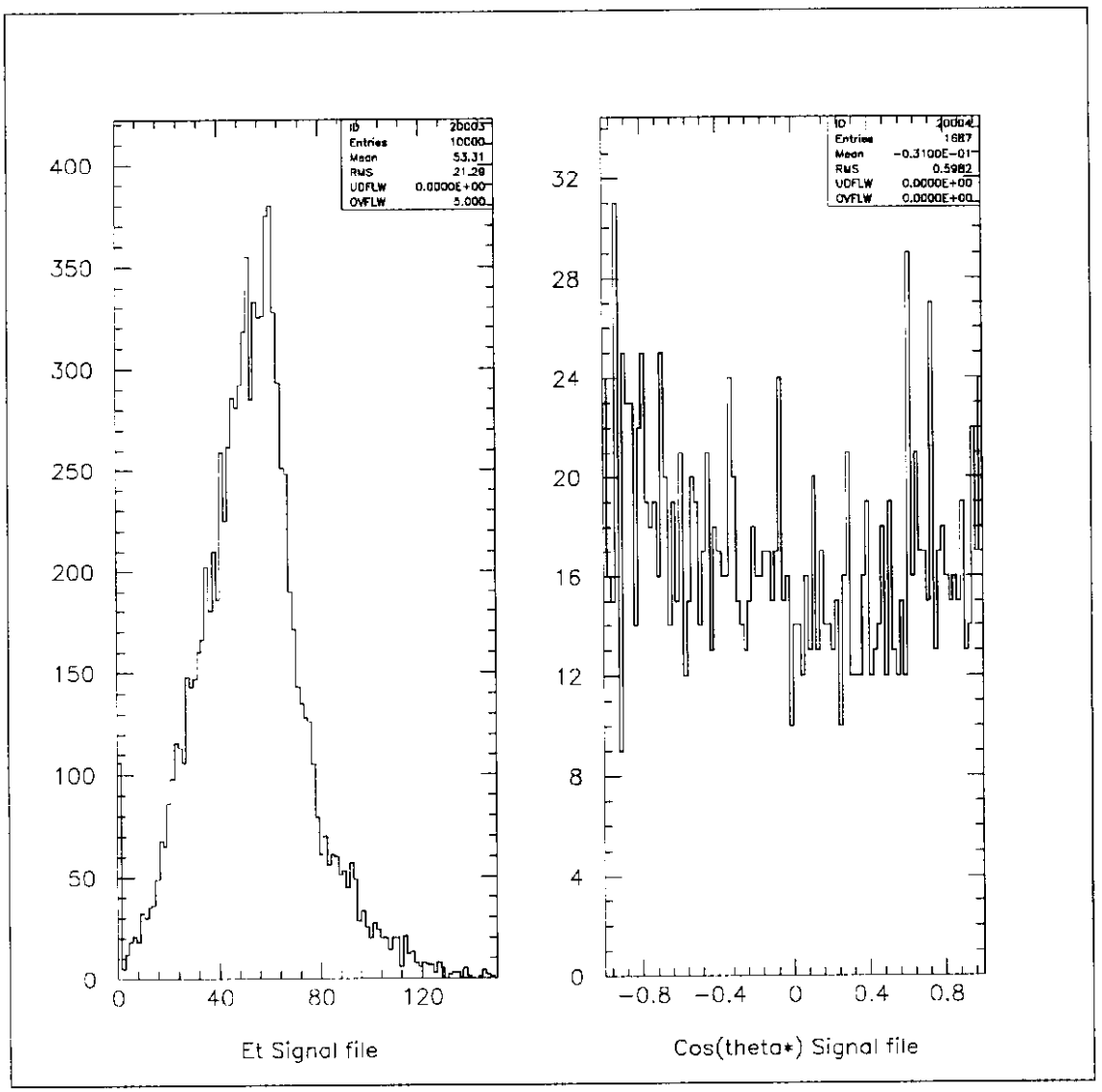


**Figure : 3.3 Distribution of $E_T$ for $H \rightarrow \gamma\gamma$ Fig. 3.4 Distribution of $\cos(\theta^*)$ for $H \rightarrow \gamma\gamma$**

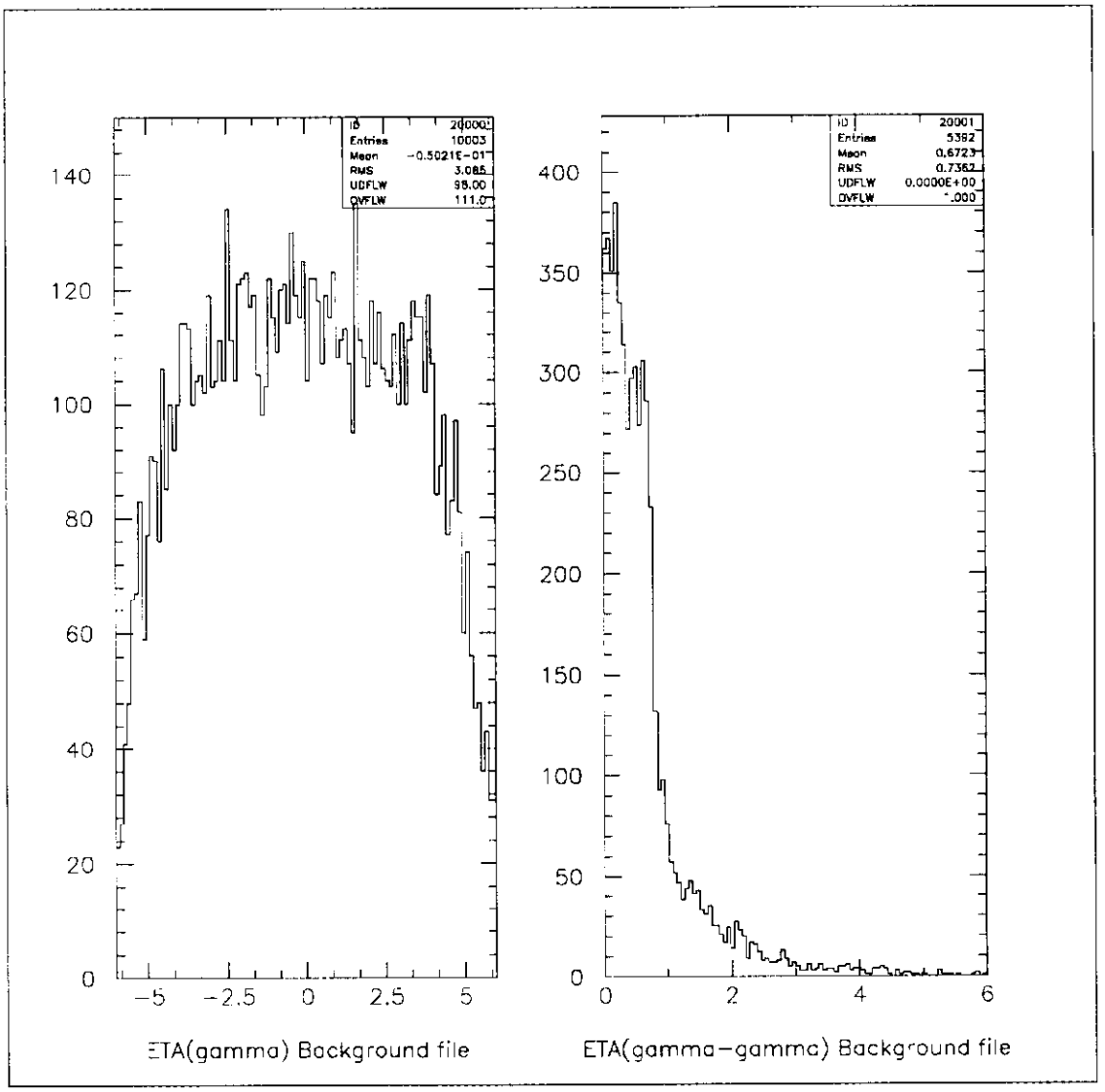


**Figure : 4.1 Distribution of $\eta_\gamma$ for $q\bar{q} \rightarrow \gamma\gamma$ Fig. 4.2 Distribution of $\eta_{\gamma\gamma}$ for $q\bar{q} \rightarrow \gamma\gamma$**

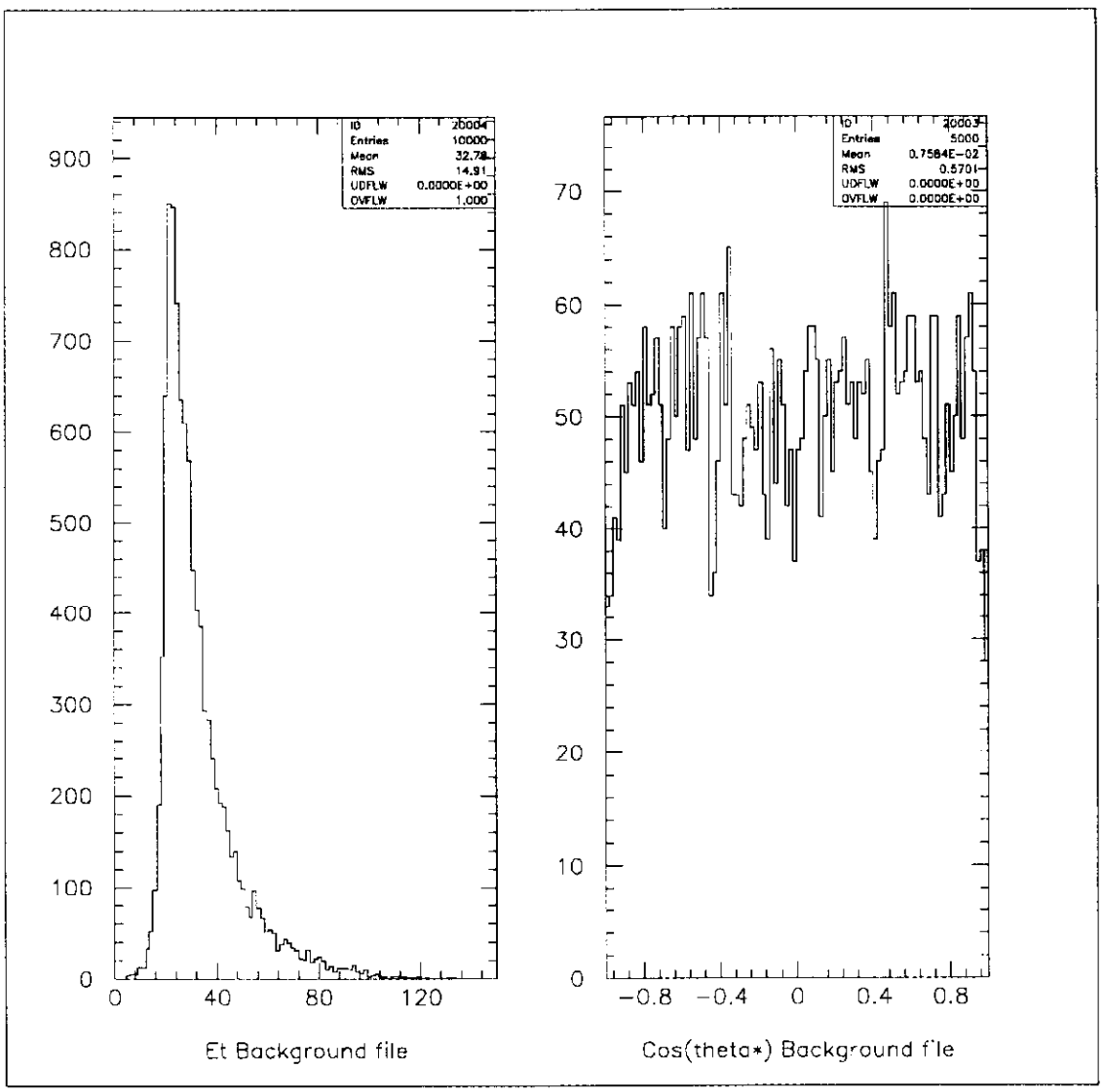


**Figure : 4.3 Distribution of $E_T$ for $q\bar{q} \rightarrow \gamma\gamma$ Fig. 4.4 Distribution of $\cos(\theta^*)$ for $q\bar{q} \rightarrow \gamma\gamma$**

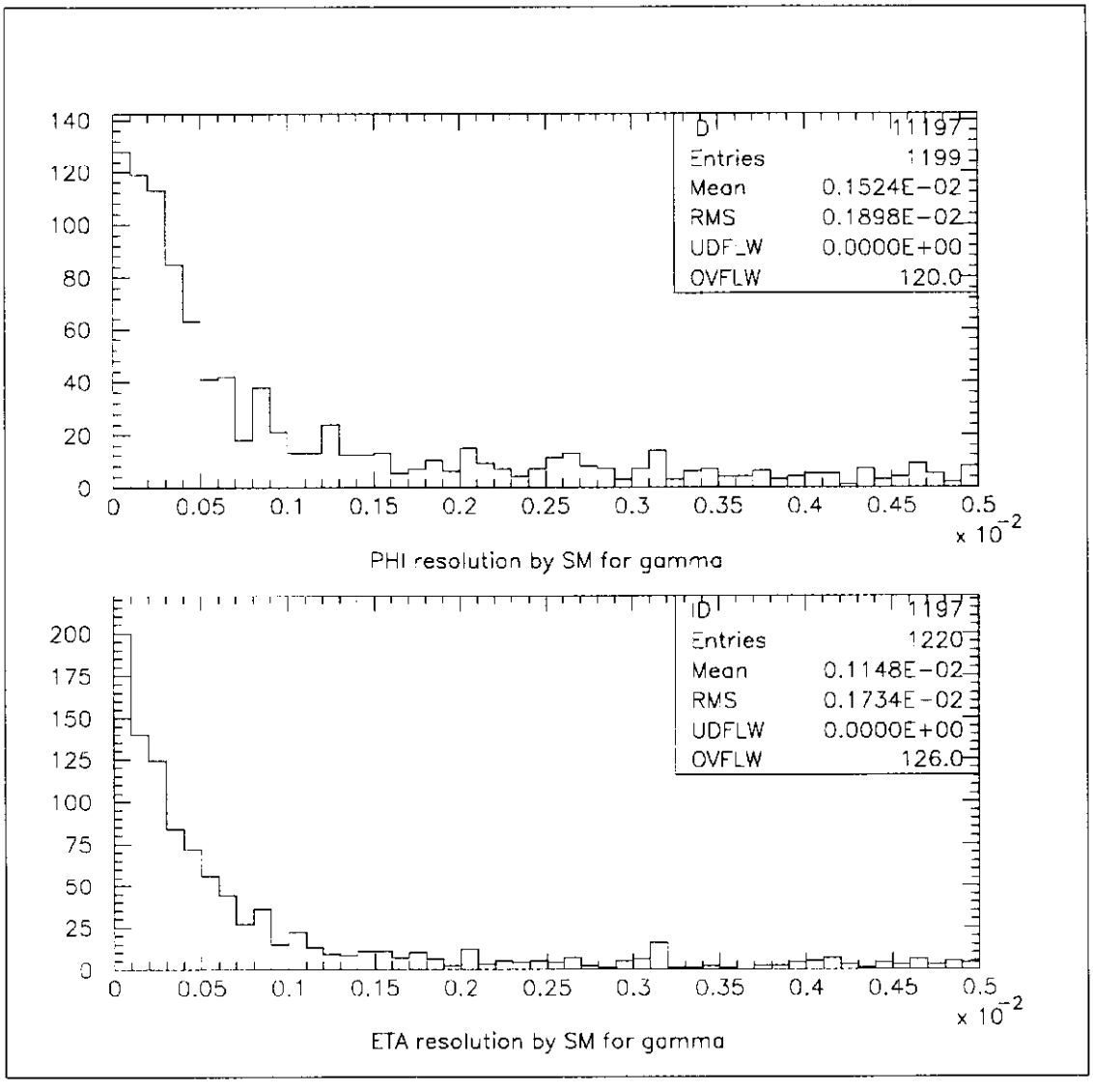


**Figure : 5 The $\phi$ and $\eta$ resolution for a Shower Maximum (SM) detector.**

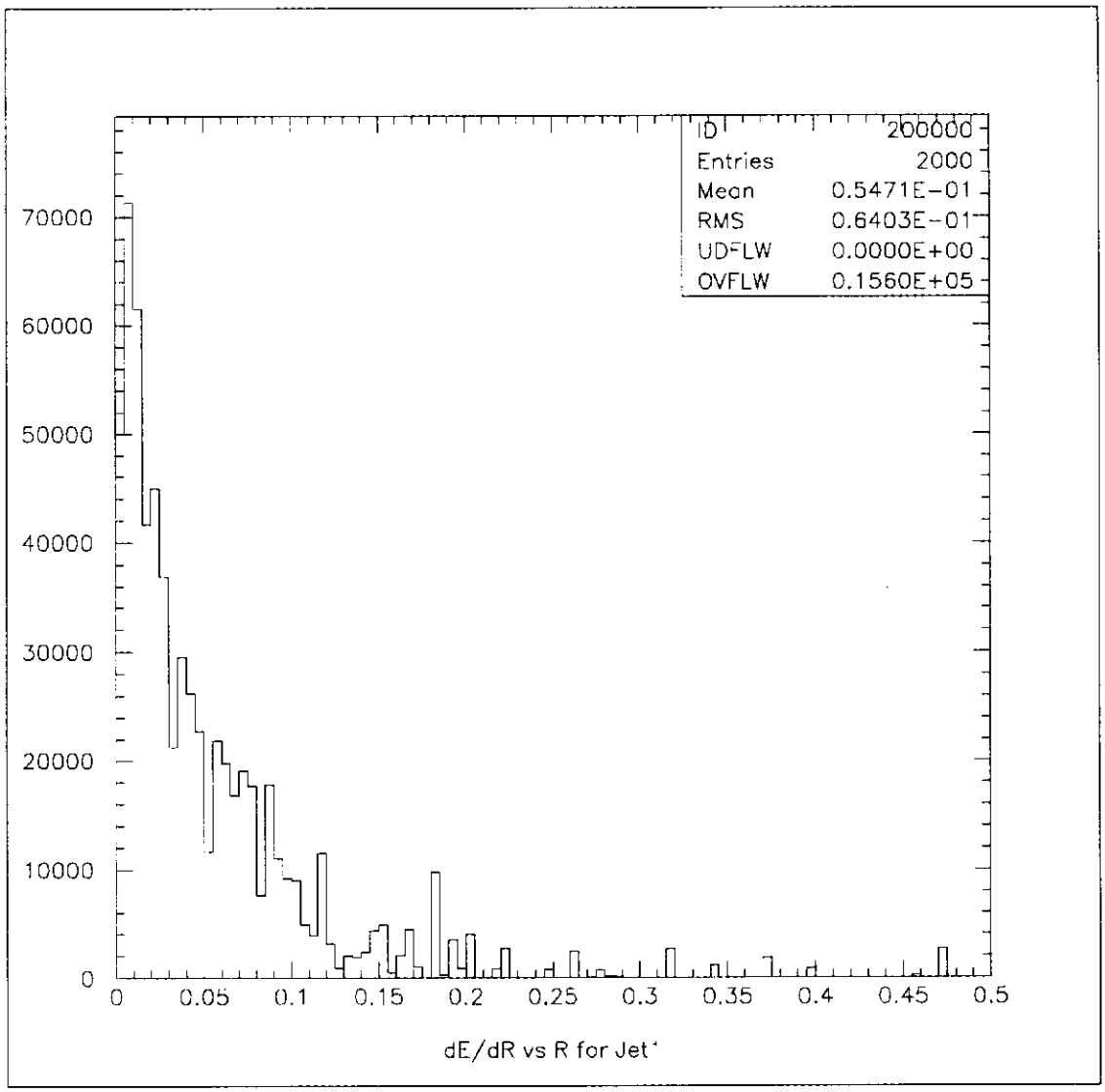


**Figure : 6 Histogram of $\frac{dE}{dR}$ versus R for a conventional resolution calorimeter.**

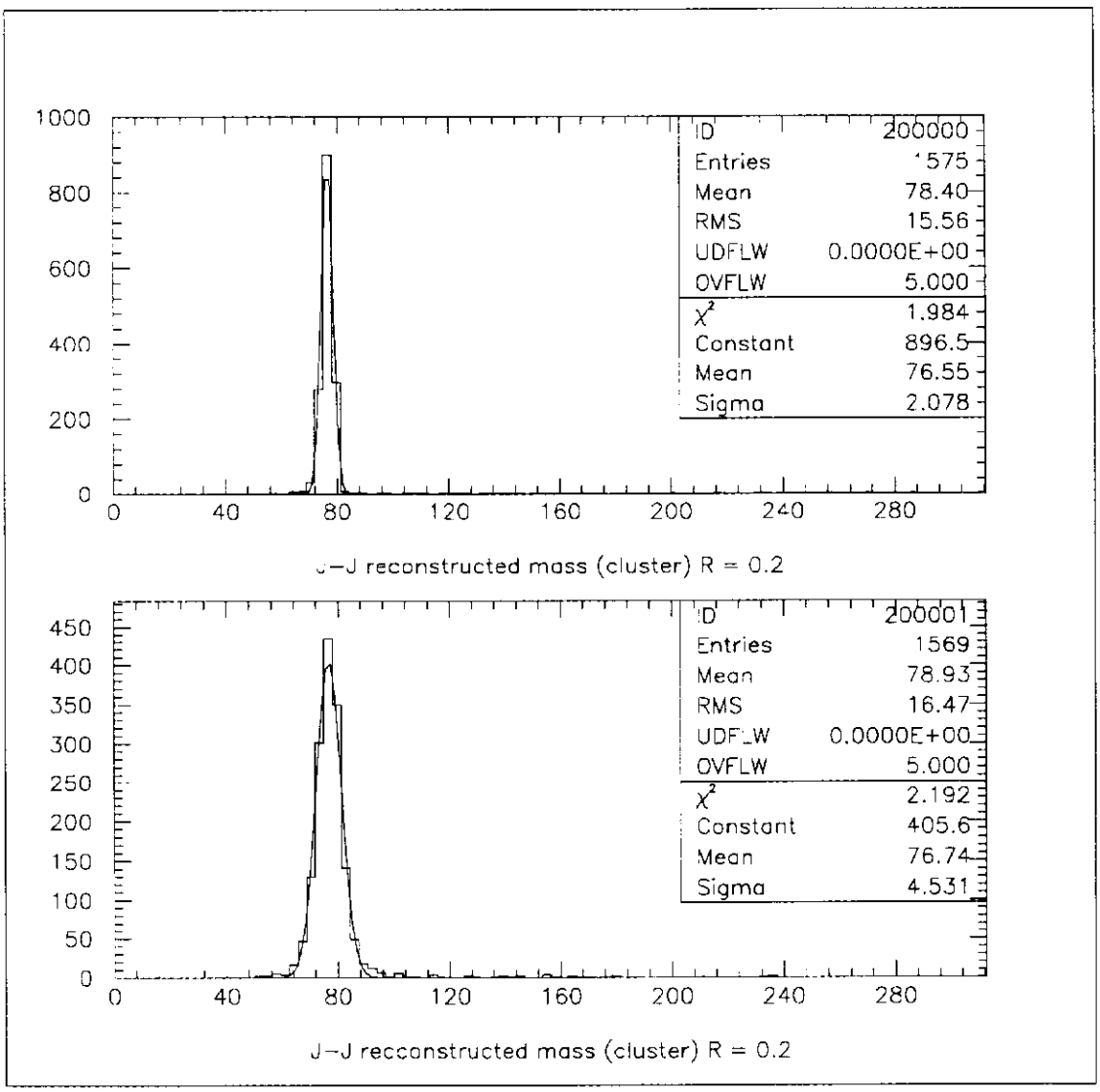


Figure : 7.1 (7.2) Higgs mass as reconstructed from two clusters by a Super (Conventional) Resolution calorimeter. The Higgs mass was generated at 80 GeV/$c^2$.

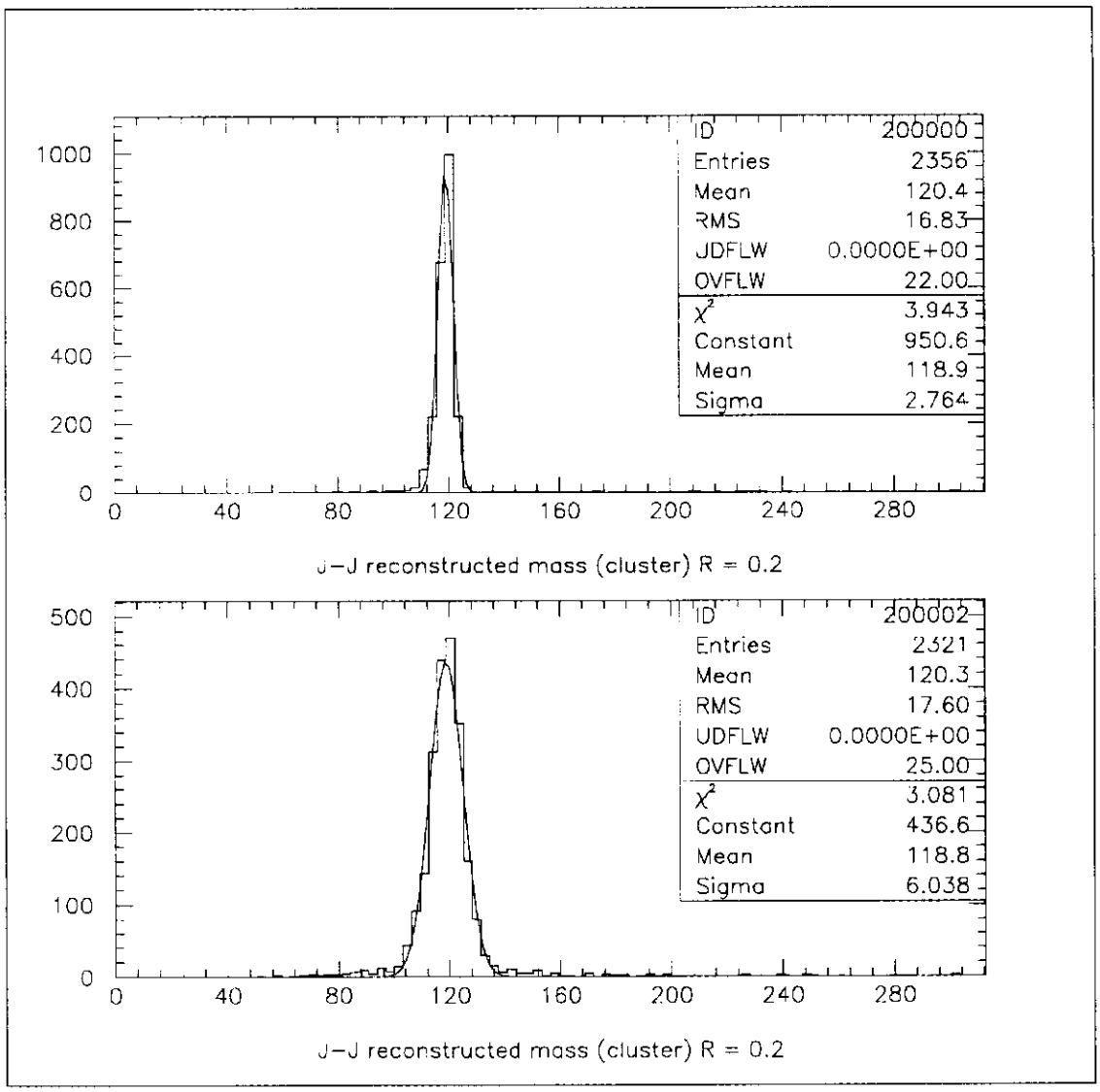


Figure : 8.1 (8.2) Higgs mass as reconstructed from two clusters by a Super (Conventional) Resolution calorimeter. The Higgs mass was generated at 125 GeV/$c^2$.

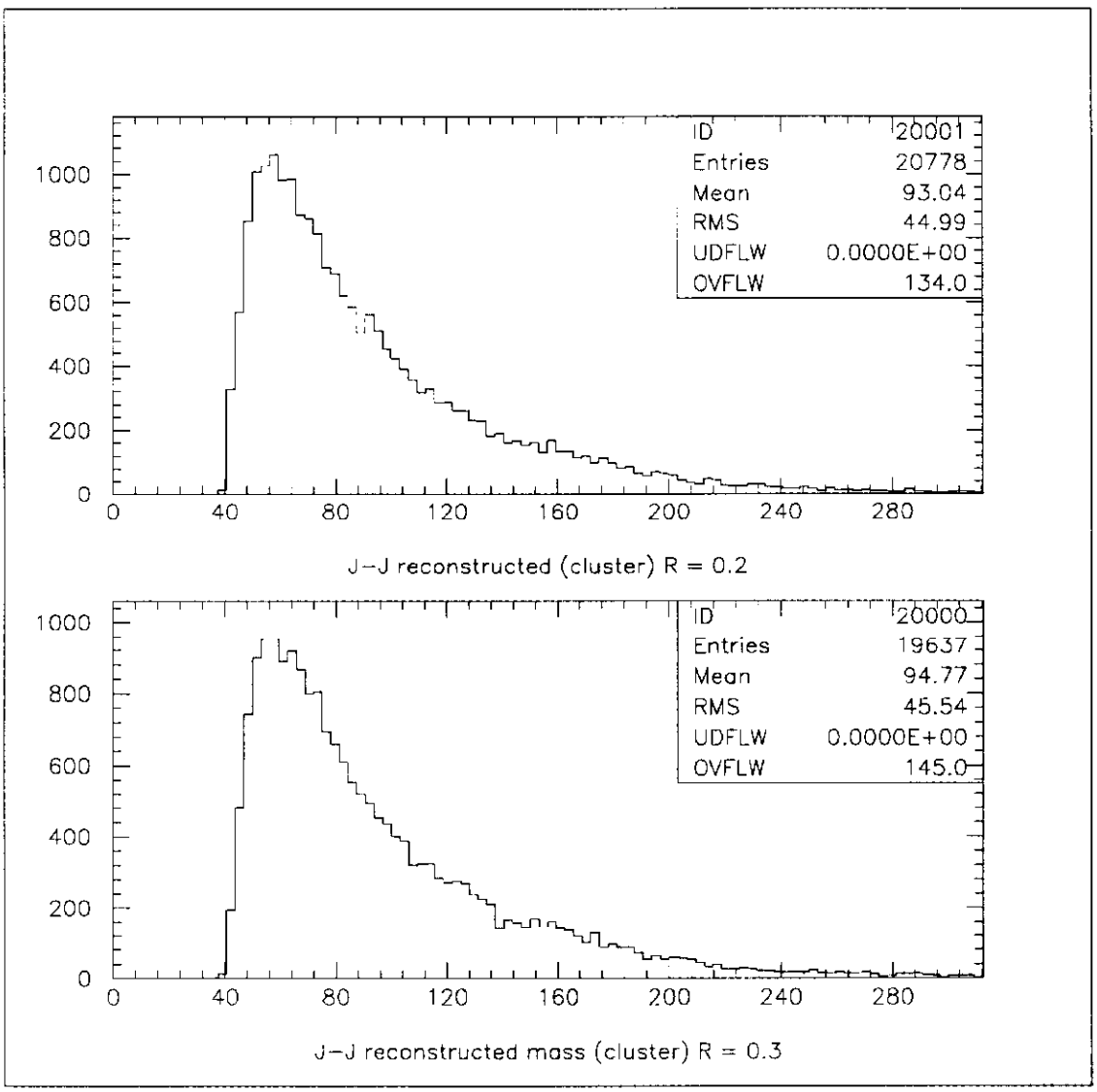


Figure : 9.1 (9.2) Mass as reconstructed from two clusters by a Super (Conventional) Resolution calorimeter. The clusters were generated by $\gamma$'s produced from $q\bar{q} \rightarrow \gamma\gamma$.

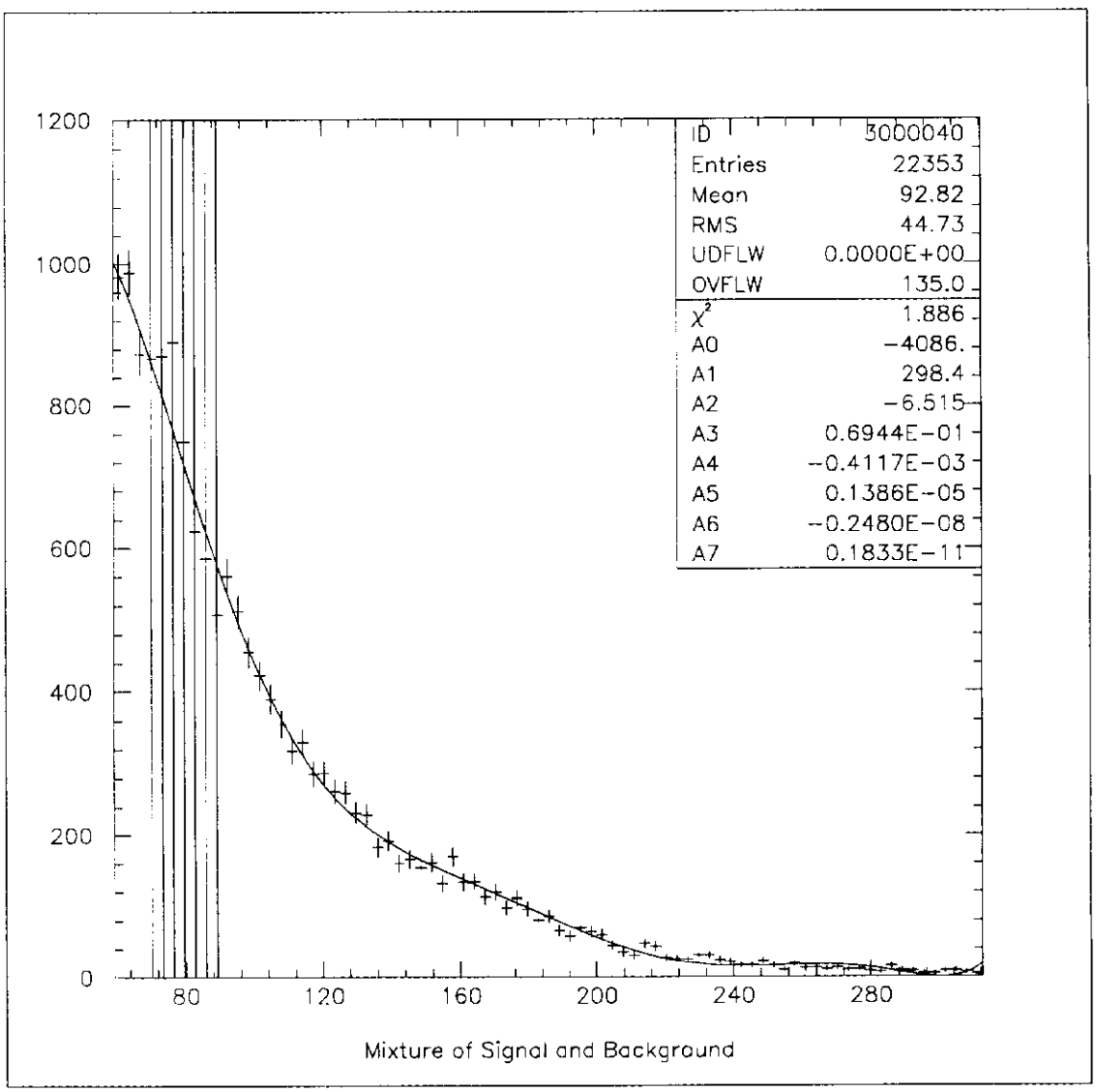


Figure : 10.1 Mass as reconstructed from two clusters in the Calorimeter (Super Resolution). The clusters were generated using a signal (Higgs mass of 80 GeV/$c^2$) of 1000 events and a background of 100,000 events. A smooth curve shows a fit to the background.

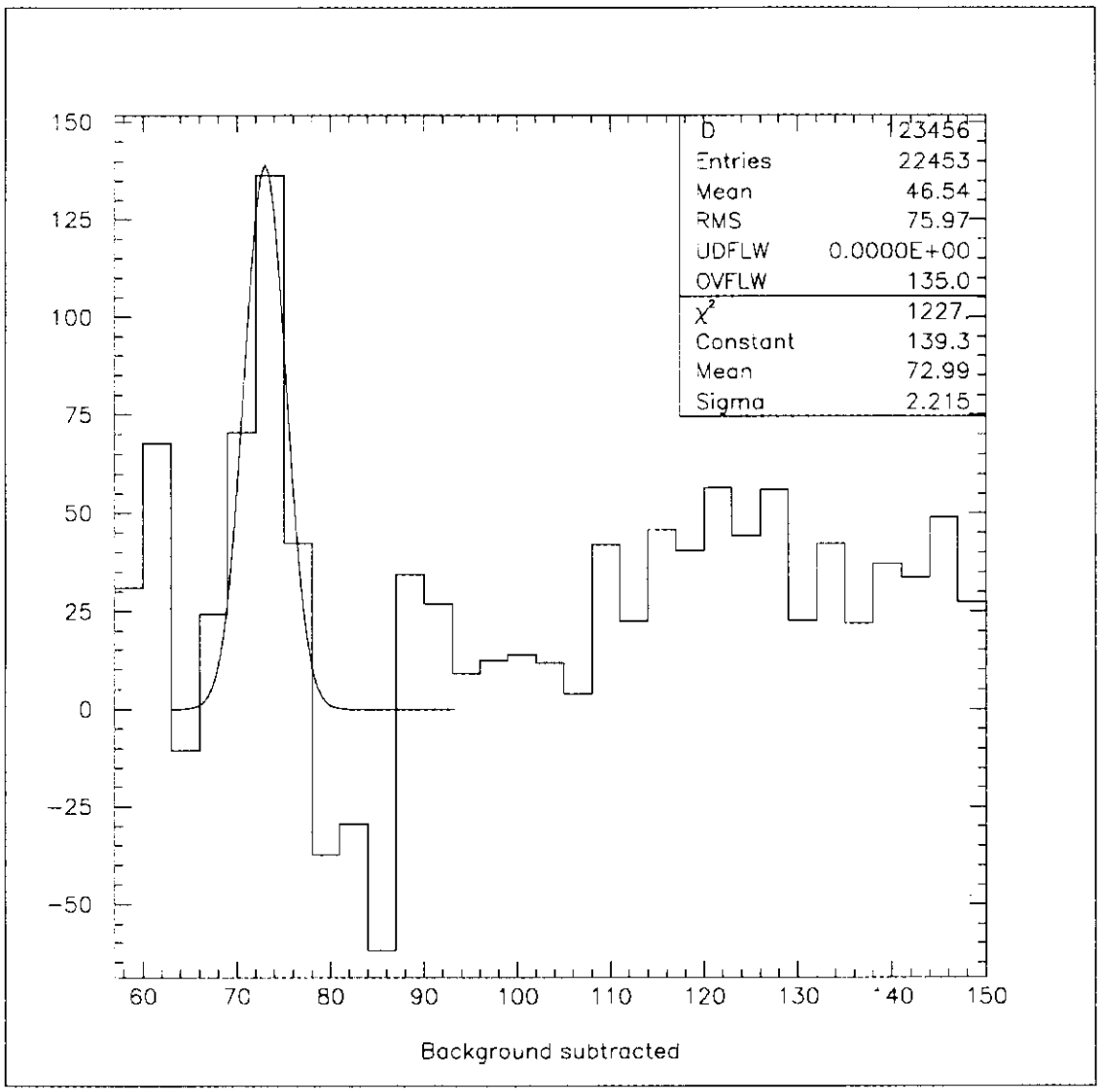


Figure : 10.2 A histogram of the Higgs mass distribution after the background given in Fig. 9.1 has been subtracted. A Gaussian fit to the signal gives a mean of 73.0 GeV and $\sigma$ of 2.2 GeV.

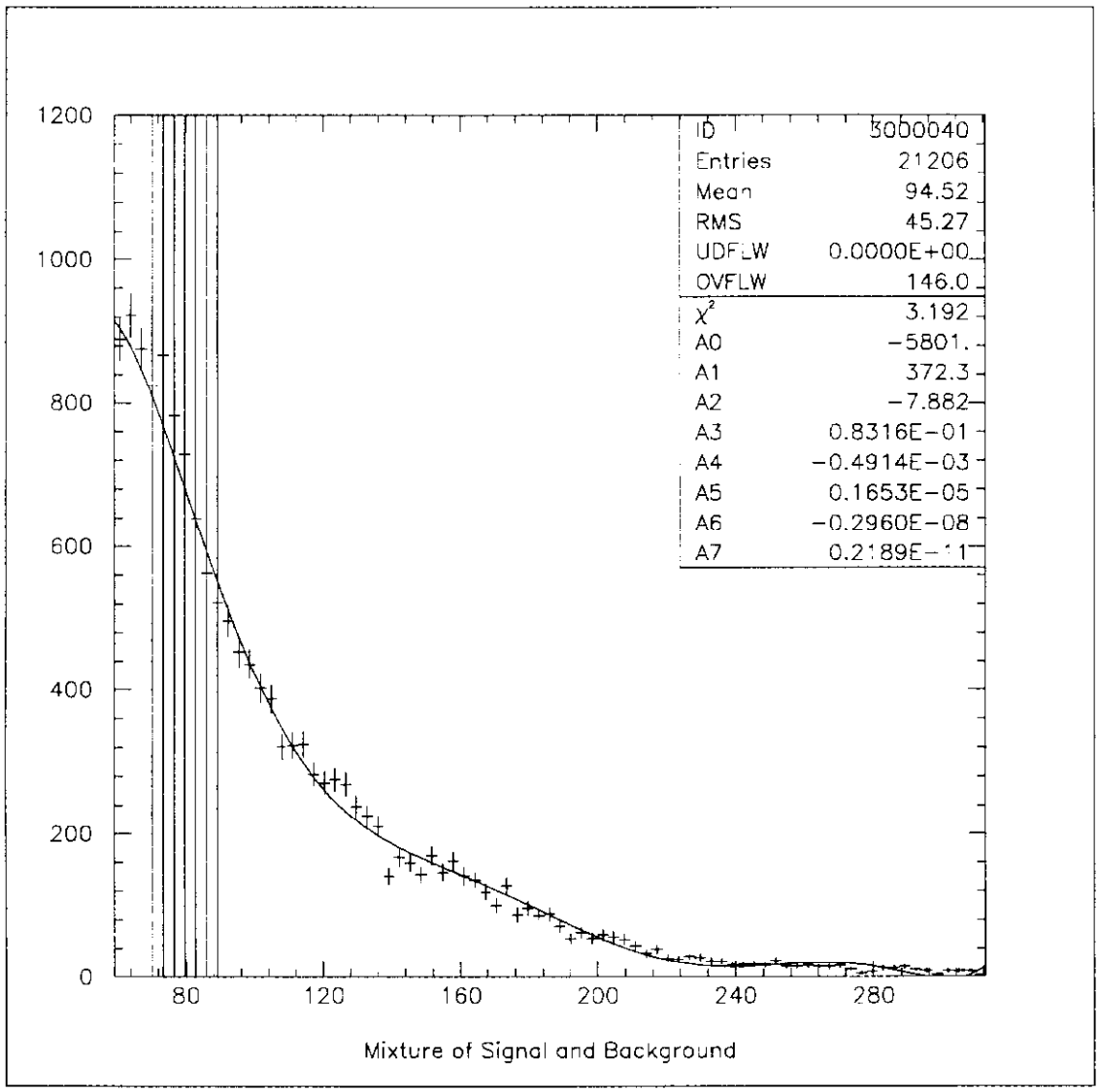


Figure : 11.1 Mass as reconstructed from two clusters in the Calorimeter (Conventional Resolution). The clusters were generated using a signal (Higgs mass of 80 GeV/$c^2$) of 1000 events and a background of 100,000 events. A smooth curve shows a fit to the background.

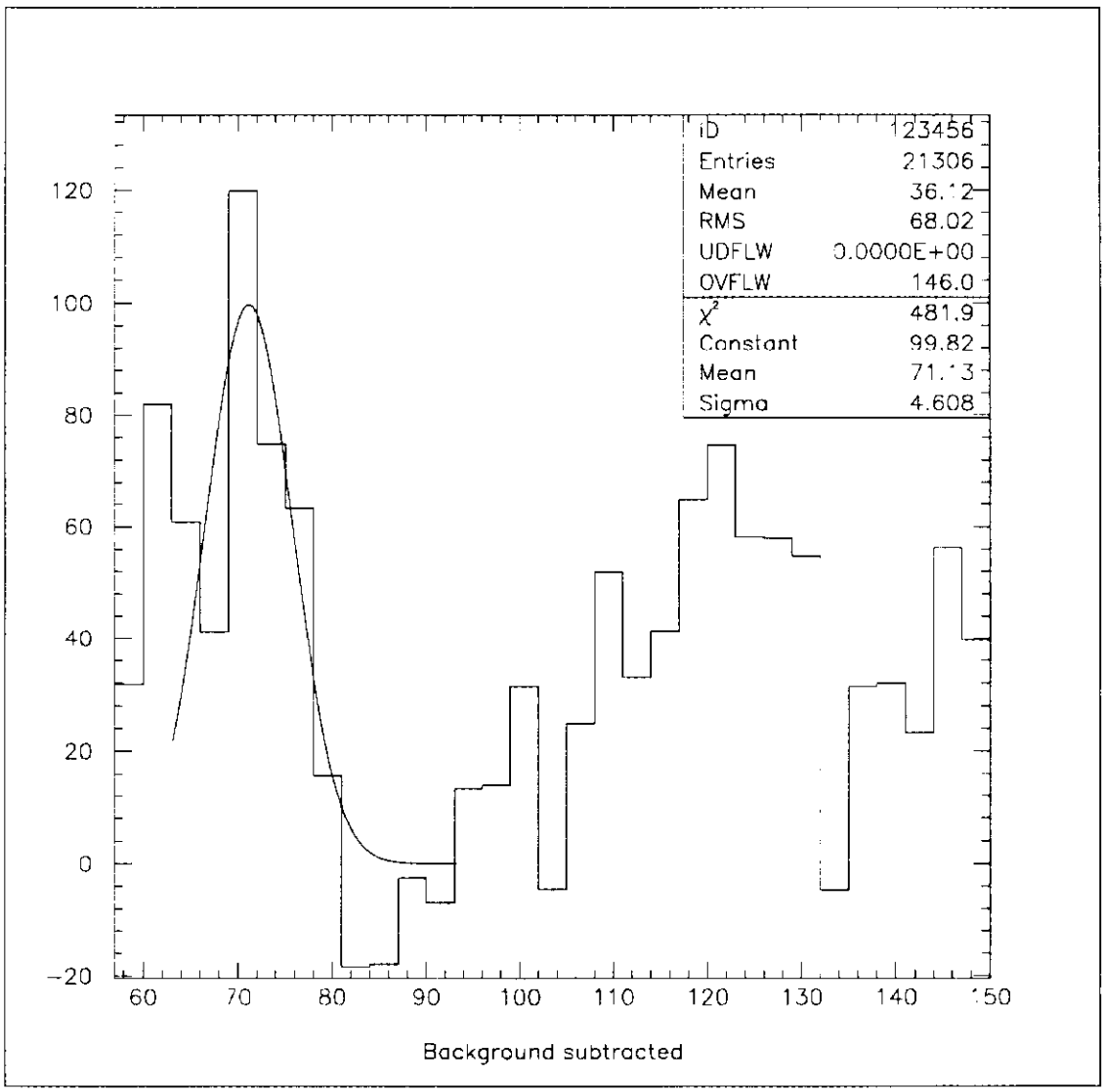


Figure : 11.2 A histogram of the Higgs mass distribution after the background given in Fig. 10.1 has been subtracted. A Gaussian fit to the signal gives a mean of 71.1 GeV and $\sigma$ of 4.6 GeV.

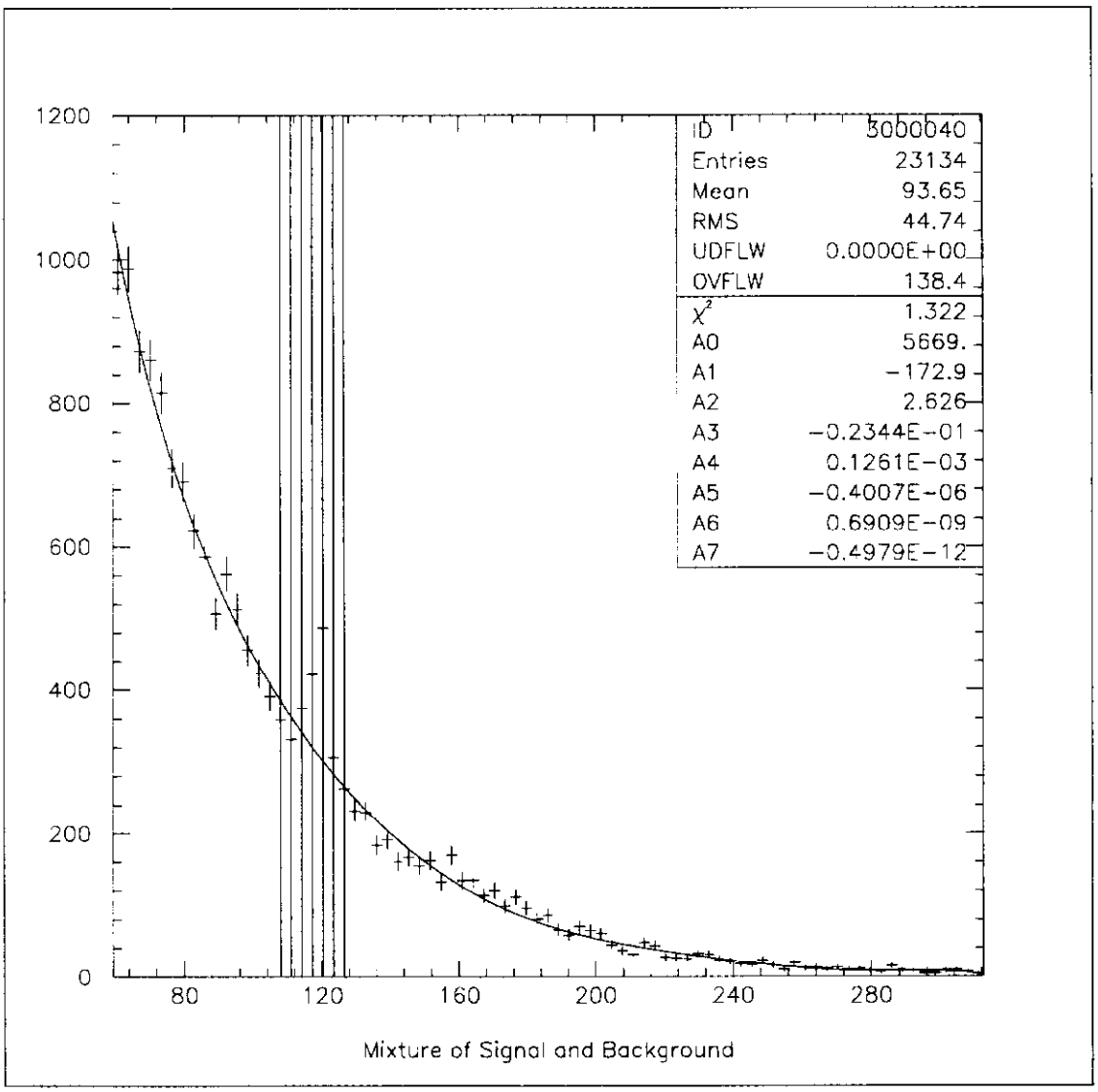


Figure : 12.1 Mass as reconstructed from two clusters in the Calorimeter (Super Resolution). The clusters were generated using a signal (Higgs mass of 1250 GeV/$c^2$) of 1000 events and a background of 100,000 events. A smooth curve shows a fit to the background.

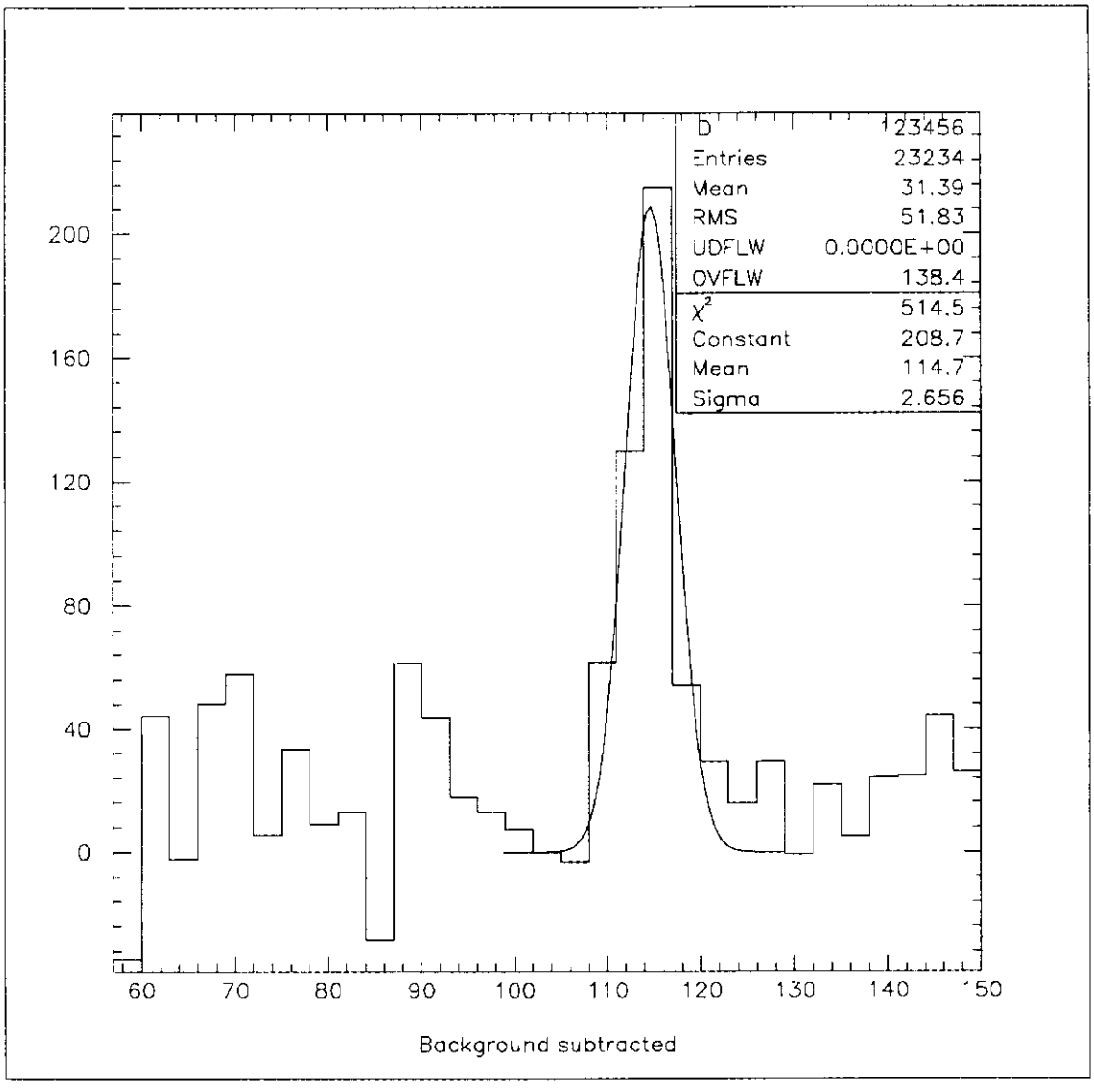


Figure : 12.2 A histogram of the Higgs mass distribution after the background given in Fig. 11.1 has been subtracted. A Gaussian fit to the signal gives a mean of 114.7 GeV and $\sigma$ of 2.7 GeV.

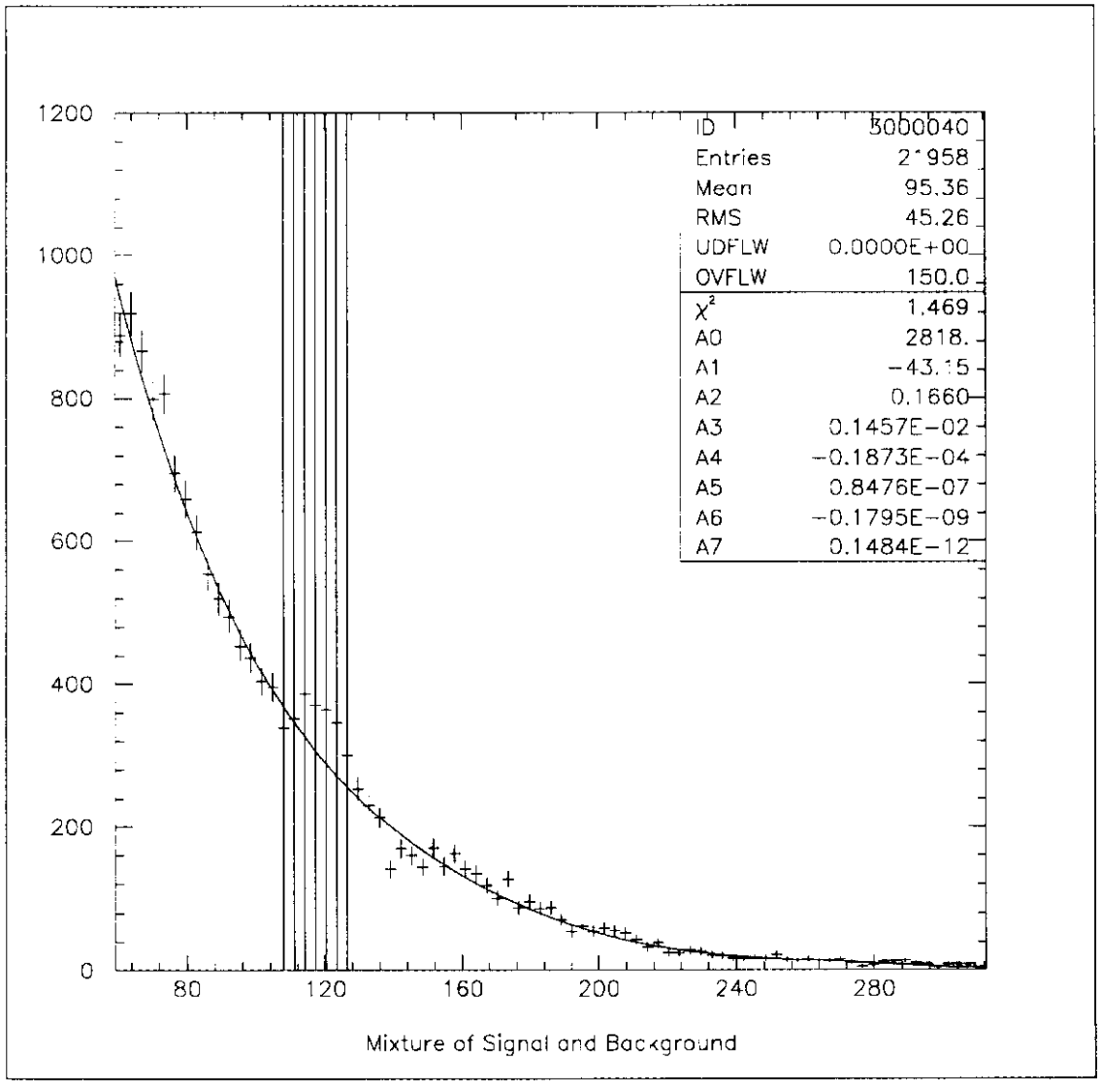


Figure : 13.1 Mass as reconstructed from two clusters in the Calorimeter (Conventional Resolution). The clusters were generated using a signal (Higgs mass of 125 GeV/$c^2$) of 1000 events and a background of 100,000 events. A smooth curve shows a fit to the background.

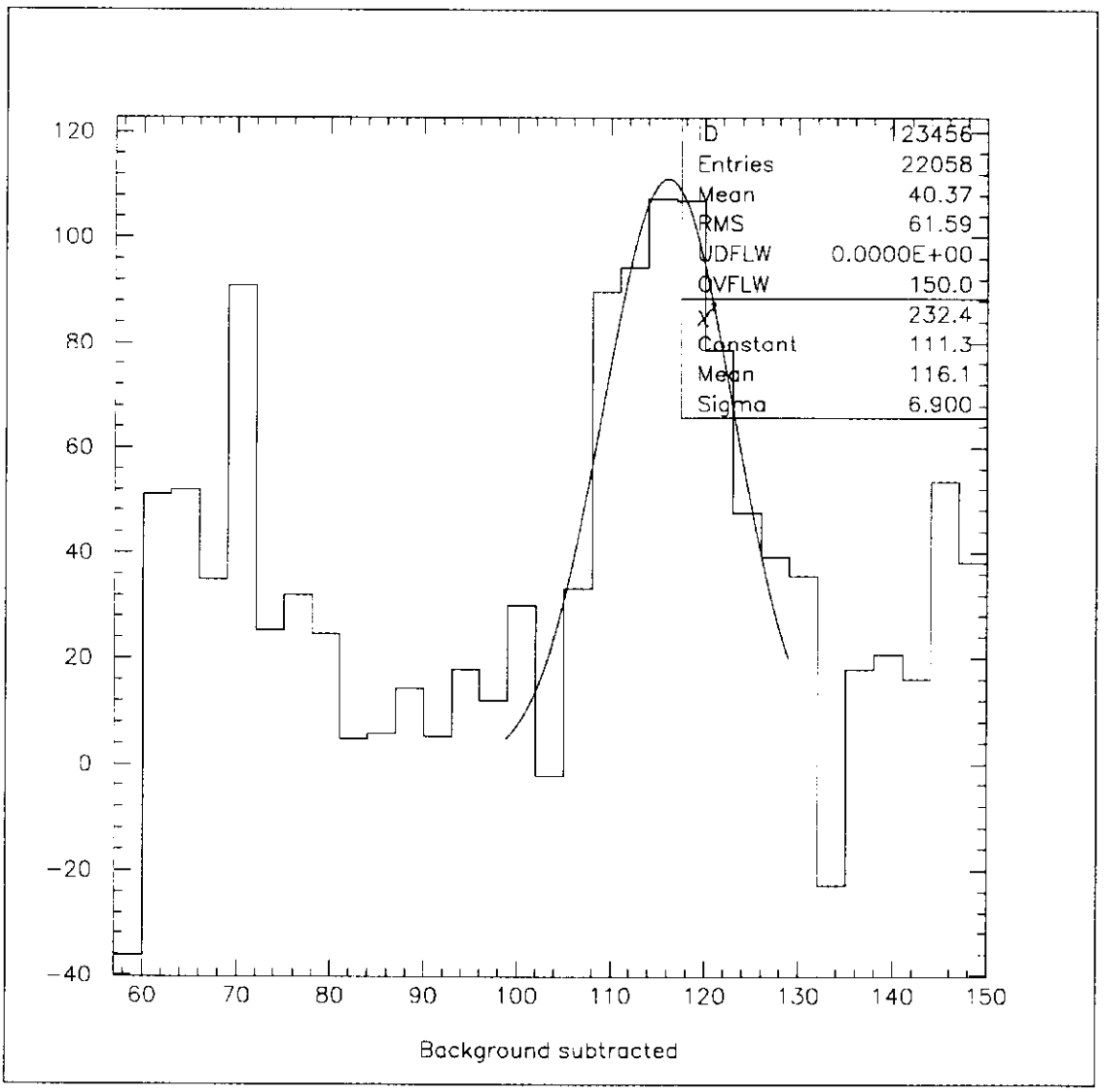


Figure : 13.2 A histogram of the Higgs mass distribution after the background given in Fig. 12.1 has been subtracted. A Gaussian fit to the signal gives a mean of 116.1 GeV and $\sigma$ of 6.9 GeV.